2024 European Control Conference (ECC)
June 25-28, 2024. Stockholm, Sweden

Interaction-aware Traffic Prediction and Scenario-based Model Predictive Control for Autonomous Vehicles on Highways*

Xiaorong Zhang[1], Sahar Zeinali[1], and Georg Schildbach[1]

Abstract— **This paper addresses the problem of traffic prediction and control of autonomous vehicles on highways. A modified Interacting Multiple Model Kalman filter algorithm is applied to predict the motion behavior of the traffic participants by considering their interactions. A scenario generation component is used to produce plausible scenarios of the vehicles based on the predicted information. A novel integrated decision-making and control system is proposed by applying a Scenario-based Model Predictive Control approach. The designed controller considers safety, driving comfort, and traffic rules. The recursive feasibility of the controller is guaranteed under the inclusion of the 'worst case' as an additional scenario to obtain safe inputs. Finally, the proposed scheme is evaluated using the HighD dataset. Simulation results indicate that the vehicle performs safe maneuvers in different traffic situations under the designed control framework.**

I. INTRODUCTION

A. Motivation

Designing control systems for autonomous vehicles on highways has been extensively studied in recent decades. These systems primarily aim to safely control the ego vehicle (EV) by predicting the motion states of the surrounding target vehicles (TVs) [1]. The predicted states are usually uncertain, so generating safe, comfortable, energy-efficient, and real-time capable control strategies is challenging.

B. Literature Review

Interaction-aware motion prediction is widely investigated since it can represent realistic traffic scenarios, and controlling the EV under interaction-aware scenarios makes the EV safer [2]. Model Predictive Control (MPC) has been extensively applied to control the EV based on the predicted motions of TVs [3]. The predictions can be used to formulate explicit constraints within the MPC to compute collision-free EV actions. As a variant of Stochastic MPC, Scenario-based MPC (SCMPC) has been successfully implemented in various highway traffic conditions, as it is easily compatible with the traffic prediction component and can handle uncertainty using limited scenarios [4]. To model the interaction between vehicles over the MPC prediction horizon, the EV's motion is modeled as a stochastic process, and the mode transition is modeled as a Markov chain in [5] [6]. The transition model is either learned or estimated using the previous EV and TVs measurements. A stochastic safety guarantee for the EV is introduced in [7] based on the TVs' motion behavior, where a set of possible TV trajectories is obtained by training the predictive model in a given scenario. A Branch MPC is proposed in [8], where a scenario tree and a trajectory tree are applied to represent the possible motion behavior of the EV and TVs. The branch probability of two trees influences each other based on their interactions. In another approach, a trajectory prediction method is represented by learning the fused EV and TVs model considering their inner influence inside MPC [9].

Safety is one of the most critical aspects of controlling the EV. This feature becomes more challenging in emergency scenarios, e.g., unexpected deceleration of the leading vehicle (LV) or a sudden cut-in of a TV. These circumstances are identified as a safety-critical-event (SCE), where the EV immediately brakes against the crash, which may lead to a deceleration until a standstill [10]. Adaptive Cruise Control (ACC) is a helpful tool for solving SCEs, where the EV reacts based on information about the LV. However, a large time headway in this algorithm may lead to over-conservative actions [11]. A safety controller is proposed based on ACC in [12], where the EV uses a predefined deceleration profile. Another representative solution to SCEs is the rigorous formalizing mathematical model of Responsibility-Sensitive-Safety. In this model, a safety distance is defined by assuming a 'worst case' scenario, and the EV responds to an SCE by decelerating at a predefined rate without full braking. This approach might be sensitive to the parameter design, and the subtle change of the parameter set might lead to a different decision strategy [13].

C. Contribution

Considering vehicles' interaction and generating traffic scenarios within MPC make the problem complicated and computationally costly. To solve this challenge, we apply a computation-efficient Interacting Multiple Model Kalman filter (IMM-KF) to produce possible interaction-aware scenarios [14]. Then, the scenarios obtained are considered in SCMPC to compute collision-free actions for the EV. Moreover, two control modes, i.e., 'lane-keeping' and 'lane-change', are proposed to decrease the complexity of the problem by excluding the decision-making process of the EV. The safety of the EV is guaranteed by theoretically proving the recursive feasibility of the SCMPC under the 'worst case' scenario. To the best of the authors' knowledge, no work has handled all the mentioned problems with an integrated SCMPC structure while proving the feasibility of the algorithm. The proposed method is evaluated for different HighD dataset scenarios, showing that EV performs safe and

*This work was supported by the Deutsche Forschungsgemeinschaft (DFG, German Research Foundation) – project number 460891204.

[1]Institute for electrical engineering in Medicine,University of luebeck, Luebeck, Germany {xiaorong.zhang, sahar.zeinali, georg.schildbach}@uni-luebeck.de

desirable maneuvers under the designed control architecture.

II. CONTROL ARCHITECTURE

The proposed control structure in Fig. 1 works as follows. First, considering the vehicles' interaction, the TV's mode states are predicted using IMM-KF, and then are used to produce all possible traffic scenarios. The high-probability scenarios are filtered and included in formulating the safety constraints of two SCMPCs along with the 'worst case' scenario. Then, a control system consisting of 'lane-keeping' and 'lane-change' modes is established. The control input with minimal cost is chosen in the decision-making module and applied to the EV.

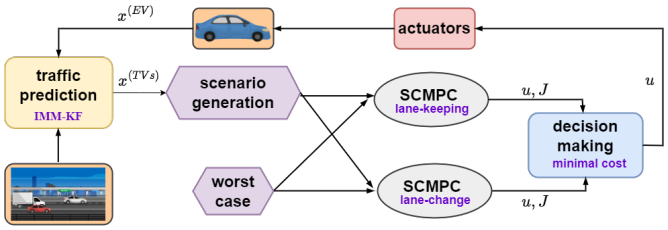

Fig. 1: Schematic diagram of the proposed control structure

III. SCENARIO GENERATION

A. Intention-based Policy Mode

In the longitudinal direction, the 'velocity tracking' (VT) and 'distance keeping' (DK) modes [14] are used. The vehicle tracks a reference velocity in VT while keeping a safe distance from its LV in DK. In the lateral direction, three modes corresponding to 'lane 1', 'lane 2', and 'lane 3' represent the target lanes of the vehicles. Thus, the total number of modes M is 6.

The common state vector x_k in all modes at time k is

$$x_k \triangleq \Big[\underbrace{p_{\text{lon},k} \quad v_{\text{lon},k} \quad a_{\text{lon},k}}_{x_{\text{lon},k}} \quad \underbrace{p_{\text{lat},k} \quad v_{\text{lat},k} \quad a_{\text{lat},k}}_{x_{\text{lat},k}}\Big]^\top, \tag{1}$$

where $p_{*,k}, v_{*,k}, a_{*,k}$ are respectively the position, velocity, and acceleration in the corresponding direction, $* \in \{\text{lon}, \text{lat}\}$. The unknown reference variable $r_{\text{ref},k}$, i.e., reference velocity $v_{\text{ref},k}$ or the reference time gap $t_{\text{gap},k}$, is also included in the longitudinal policy mode to be estimated. Therefore, the full state vector z_k in each policy mode at time k is

$$z_k \triangleq \Big[\underbrace{x_{\text{lon},k} \quad r_{\text{ref},k}}_{z_{\text{lon},k}} \quad \underbrace{x_{\text{lat},k}}_{z_{\text{lat},k}}\Big]^\top. \tag{2}$$

Note that we use $x_k^{(\circledast)}$ or $z_k^{(\circledast)}$ to clarify the common or full state of a specific vehicle, where $\circledast \in \{\text{EV, TV, LV}\}$. To make the policies closer to the driver's real intention, two linear quadratic regulator (LQR)-based feedback controllers are included in longitudinal and lateral policy modes. The associated control gains are defined as follows:

$$K_{\text{lon}}^{(\diamond)} = \begin{bmatrix} K_{\text{lon},1}^{(\diamond)} & K_{\text{lon},2}^{(\diamond)} & K_{\text{lon},3}^{(\diamond)} \end{bmatrix}^\top, \tag{3a}$$

$$K_{\text{lat}} = \begin{bmatrix} K_{\text{lat},1} & K_{\text{lat},2} & K_{\text{lat},3} \end{bmatrix}^\top. \tag{3b}$$

where $\diamond \in \{\text{VT}, \text{DK}\}$. Denoting the sampling time as T, the discrete form of each policy mode at time k is

$$\underbrace{\begin{bmatrix} z_{\text{lon},k+1} \\ z_{\text{lat},k+1} \end{bmatrix}}_{z_{k+1}} = \underbrace{\begin{bmatrix} F_{\text{lon},k}^{(\diamond)} & \mathbf{0}_{4\times3} \\ \mathbf{0}_{3\times4} & F_{\text{lat},k}^{(\lambda)} \end{bmatrix}}_{F_k} \underbrace{\begin{bmatrix} z_{\text{lon},k} \\ z_{\text{lat},k} \end{bmatrix}}_{z_k} + \underbrace{\begin{bmatrix} E_{\text{lon},k}^{(\diamond)} \\ E_{\text{lat},k}^{(\lambda)} \end{bmatrix}}_{E_k} + \omega_k, \tag{4a}$$

$$y_k = \boldsymbol{I}_{7\times7} z_k + \nu_k, \tag{4b}$$

where $y_k \in \mathbb{R}^7$ and $\boldsymbol{I}_{7\times7}$ are the measurement vector and observation matrix. ω_k and ν_k are assumed to be normally distributed process noise and measurement noise, with the covariances Q and R. The longitudinal system matrices are

$$F_{\text{lon},k}^{(\text{VT})} = \begin{bmatrix} 1 & T & \frac{T^2}{2} & 0 \\ 0 & 1 - \frac{K_{\text{lon},2}^{(\text{VT})} T^2}{2} & T - \frac{K_{\text{lon},3}^{(\text{VT})} T^2}{2} & \frac{K_{\text{lon},2}^{(\text{VT})} T^2}{2} \\ 0 & -K_{\text{lon},2}^{(\text{VT})} T & 1 - K_{\text{lon},3}^{(\text{VT})} T & K_{\text{lon},2}^{(\text{VT})} T \\ 0 & 0 & 0 & 1 \end{bmatrix},$$

$$F_{\text{lon},k}^{(\text{DK})} = \begin{bmatrix} 1 - \frac{K_{\text{lon},1}^{(\text{DK})} T^3}{6} & -\frac{K_{\text{lon},1}^{(\text{DK})} T^2}{2} & -K_{\text{lon},1}^{(\text{DK})} T & 0 \\ T - \frac{K_{\text{lon},2}^{(\text{DK})} T^3}{6} & 1 - \frac{K_{\text{lon},2}^{(\text{DK})} T^2}{2} & -K_{\text{lon},2}^{(\text{DK})} T & 0 \\ \frac{T^2}{2} - \frac{K_{\text{lon},3}^{(\text{DK})} T^3}{6} & T - \frac{K_{\text{lon},3}^{(\text{DK})} T^2}{2} & 1 - K_{\text{lon},3}^{(\text{DK})} T & 0 \\ -\frac{K_{\text{lon},1}^{(\text{DK})} v_{\text{lead},k} T^3}{6} & -\frac{K_{\text{lon},1}^{(\text{DK})} v_{\text{lead},k} T^2}{2} & -K_{\text{lon},2}^{(\text{DK})} v_{\text{lead},k} T & 1 \end{bmatrix}^\top,$$

and the LQR-related input matrices are

$$E_{\text{lon},k}^{(\text{VT})} = \mathbf{0}_{4\times1},$$

$$E_{\text{lon},k}^{(\text{DK})} = \begin{bmatrix} \frac{K_{\text{lon},1}^{(\text{DK})} T^3}{6} - 1 & \frac{K_{\text{lon},2}^{(\text{DK})} T^3}{6} - T & \frac{K_{\text{lon},3}^{(\text{DK})} T^3}{6} - \frac{T^2}{2} & 0 \\ \frac{K_{\text{lon},1}^{(\text{DK})} T^2}{2} & \frac{K_{\text{lon},2}^{(\text{DK})} T^2}{2} - 1 & \frac{K_{\text{lon},3}^{(\text{DK})} T^2}{2} - T & 0 \\ K_{\text{lon},1}^{(\text{DK})} T & K_{\text{lon},2}^{(\text{DK})} T & K_{\text{lon},3}^{(\text{DK})} T - 1 & 0 \\ 0 & 0 & 0 & 0 \end{bmatrix} \begin{bmatrix} p_{\text{lon},k}^{(\text{LV})} \\ v_{\text{lon},k}^{(\text{LV})} \\ a_{\text{lon},k}^{(\text{LV})} \\ 0 \end{bmatrix}.$$

Consider the position $p^{(\lambda)}$ of the center line of the target lane λ, $\lambda = 1, 2, 3$. The lateral system and input matrices are

$$F_{\text{lat},k}^{(\lambda)} = \begin{bmatrix} -\frac{K_{\text{lat},1} T^3}{6} & -\frac{K_{\text{lat},2} T^3}{6} & -\frac{K_{\text{lat},3} T^3}{6} \\ -\frac{K_{\text{lat},1} T^2}{2} & -\frac{K_{\text{lat},2} T^2}{2} & -\frac{K_{\text{lat},3} T^2}{2} \\ -K_{\text{lat},1} T & -K_{\text{lat},2} T & -K_{\text{lat},3} T - 1 \end{bmatrix}, \tag{5a}$$

$$E_{\text{lat},k}^{(\lambda)} = \begin{bmatrix} \frac{K_{\text{lat},1} T^3}{6} p^{(\lambda)} \\ \frac{K_{\text{lat},1} T^2}{2} p^{(\lambda)} \\ K_{\text{lat},1} T p^{(\lambda)} \end{bmatrix}. \tag{5b}$$

B. Interaction-aware Estimation and Prediction

Each vehicle's state estimation and prediction are calculated in descending priority order based on vehicles' interactions. The priority criteria are (i) if two vehicles are in the same lane, the preceding one has higher priority (ii) if two vehicles are in different lanes, the one with the higher longitudinal progress over a specific horizon has higher priority [14].

For the sake of clarity, a policy mode corresponds to one model of the IMM-KF in this work. In the IMM-KF,

we consider the Markov jump linear system (4), where the transition probability from mode i to mode j is denoted as $\pi^{(i|j)}$, and $\pi^{(i|j)} \in [0,1]$, $i,j \in \{1,2,...,6\}$. Since the reference parameters of the VT and DK modes are different, we mix individual common estimates and initialize each mode in the first step as:

$$c^{(i)} = \sum_{j=1}^{M} \pi^{(j|i)} \mu_{k-1}^{(j)}, \tag{6a}$$

$$\mu_{k-1}^{(j|i)-} = \frac{\pi^{(j|i)} \mu_{k-1}^{(j)}}{c^{(i)}}, \tag{6b}$$

$$\bar{x}_{k-1}^{(i)-} = \sum_{j=1}^{M} \mu_{k-1}^{(j|i)-} \hat{x}_{k-1}^{(j)-}, \tag{6c}$$

$$\begin{aligned} \bar{P}_{k-1}^{(i)-} = \sum_{j=1}^{M} \mu_{k-1}^{(j|i)-} \Big[& P_{k-1}^{(j)-} \\ & + \left(\bar{x}_{k-1}^{(i)-} - \hat{x}_{k-1}^{(j)-}\right) \left(\bar{x}_{k-1}^{(i)-} - \hat{x}_{k-1}^{(j)-}\right)^{\top} \Big], \end{aligned} \tag{6d}$$

where $\mu_{k-1}^{(j|i)-}$ is the mixing conditional mode probability, $\hat{x}_{k-1}^{(j)-}$, $P_{k-1}^{(j)-}$ are the common state estimation and covariance, which are part of the full state estimation $\hat{z}_{k-1}^{(j)-}$, and covariance $\mathbb{P}_{k-1}^{(j)-}$. The fused common state estimation and covariance are $\bar{x}_{k-1}^{(i)-}$ and $\bar{P}_{k-1}^{(i)-}$. $\bar{z}_{k-1}^{(i)-}$ and $\bar{\mathbb{P}}_{k-1}^{(i)-}$ are fused full state estimation and covariance. Then, each mode is predicted and updated as

$$\hat{z}_{k-1}^{(i)+} = F_{k-1}^{(i)} \bar{z}_{k-1}^{(i)-} + E_{k-1}^{(i)}, \tag{7a}$$

$$\mathbb{P}_{k-1}^{(i)+} = F_{k-1}^{(i)} \bar{\mathbb{P}}_{k-1}^{(i)-} F_{k-1}^{(i)\top} + Q_{k-1}^{(i)}, \tag{7b}$$

$$\tilde{y}_k^{(i)} = y_k^{(i)} - \boldsymbol{I}_{7\times 7} \hat{z}_{k-1}^{(i)+}, \tag{7c}$$

$$r_k^{(i)} = \boldsymbol{I}_{7\times 7} \mathbb{P}_{k-1}^{(i)+} \boldsymbol{I}_{7\times 7}^{\top} + R_k^{(i)}, \tag{7d}$$

$$L_k^{(i)} = \mathbb{P}_{k-1}^{(i)+} \boldsymbol{I}_{7\times 7}^{\top} r_k^{(i)^{-1}}, \tag{7e}$$

$$\hat{z}_k^{(i)-} = \hat{z}_{k-1}^{(i)+} + L_k^{(i)} \tilde{y}_k^{(i)}, \tag{7f}$$

$$\mathbb{P}_k^{(i)-} = (\boldsymbol{I}_{7\times 7} - L_k^{(i)} \boldsymbol{I}_{7\times 7}) \mathbb{P}_{k-1}^{(i)+}, \tag{7g}$$

with the prior state estimate $\hat{z}_{k-1}^{(i)+}$ and covariance $\mathbb{P}_{k-1}^{(i)+}$, the innovation residual $\tilde{y}_k^{(i)}$ and its covariance $r_k^{(i)}$, Kalman gain $L_k^{(i)}$, and posterior predicted state estimate $\hat{z}_k^{(i)-}$ and covariance $\mathbb{P}_k^{(i)-}$. The state prediction of each mode is

$$\hat{z}_{t|k} = \phi(t,1)\hat{z}_k^{-} + \sum_{\delta=k+1}^{t} \phi(t,\delta) E_{\delta-1}, \tag{8a}$$

$$\phi(t,\delta) = \begin{cases} (\Pi_{\eta=\delta}^{t-1} F_{\eta}^{\top})^{\top} & \text{if } t > \delta \\ \boldsymbol{I}_{7\times 7}, & \text{if } t = \delta \end{cases}, \tag{8b}$$

where $t = k+1, ..., k+1+N$, N is the prediction horizon. To obtain a no-collision prediction, a mixed integer quadratic programming (MIQP) problem is formulated to modify the state estimation $\hat{z}_k^{(\text{proj})-}$, where the safety constraints between the studied vehicle and other vehicles which have higher priority are considered. Note that the state estimation of each policy mode is still $\hat{z}_k^{-}$, and only the state prediction is modified in terms of $\hat{z}_k^{(\text{proj})-}$ and (8). The state estimation error between $\hat{z}_k^{-}$ and $\hat{z}_k^{(\text{proj})-}$, and its covariance are used to augment the innovation residual $\bar{y}_k^{(i)}$ and its covariance $r_k{}^{(i)}$ as $\breve{y}_k^{(i)}$ and $\breve{r}_k^{(i)}$. Then, the policy mode probability is updated based on the augmented matrices

$$\tilde{L}_k^{(i)} = \frac{\exp(-\frac{1}{2} \breve{y}_k^{(i)\top} \breve{r}_k^{(i)-1} \breve{y}_k^{(i)})}{\left|2\pi \breve{r}_k^{(i)}\right|^{1/2}}, \tag{9a}$$

$$\tilde{\mu}_k^{(i)} = \frac{c^{(i)} \tilde{L}_k^{(i)}}{\sum_{j=1}^{M} c^{(j)} \tilde{L}_k^{(j)}}. \tag{9b}$$

The final step is to mix state estimation and its covariance according to the updated probability of the individual mode

$$\hat{x}_k^{-} = \sum_{i=1}^{M} \tilde{\mu}_k^{(i)} \hat{x}_k^{(i)-}, \tag{10a}$$

$$P_k^{-} = \sum_{i=1}^{M} \tilde{\mu}_k^{(i)} [P_k^{(i)-} + (\hat{x}_k^{-} - \hat{x}_k^{(i)-})(\hat{x}_k^{-} - \hat{x}_k^{(i)-})^{\top}]. \tag{10b}$$

The updated state estimation is also modified in terms of an MIQP problem to guarantee safety over the whole prediction horizon. The readers are referred to [14] for more details.

C. Scenario Generation of TVs

A scenario is defined as a tuple of motion maneuvers for all TVs. Assuming that the number of investigated TVs is V, then a total of M^V possible scenarios can be generated. $\mu_i^{(n)}$ is the probability of TV n with the policy mode i, $i \in \{1,2,...,6\}$. Assuming statistical independence of each vehicle's no-collision prediction over the prediction horizon, then the probability of the scenario s is calculated by

$$\Pr(s) = \prod_{n=1}^{V} \mu_i^{(n)}, \quad s = 1, ..., M^V, \tag{11}$$

where $\sum_{s=1}^{M^V} \Pr(s) = 1$. To have high-probability scenarios, scenarios with a probability less than a predefined threshold $\underline{P}$ are not considered. The probability of the remaining scenarios is normalized by

$$\overline{\Pr}(s) = \frac{\Pr(s)}{1 - \sum_{\zeta=1}^{\theta} \Pr(\zeta)}, \quad s = 1, ..., M^V - \theta, \tag{12}$$

where θ is the total number of scenarios with probability less than $\underline{P}$.

IV. SCENARIO-BASED MODEL PREDICTIVE CONTROL

Based on the predicted scenarios of the TVs, a feasible trajectory for the EV is calculated by solving a constrained finite-time optimal control problem (CFTOCP) in a moving horizon fashion. The objective of the optimization problem is to follow the planned reference trajectory with minimum effort and with the consideration of safety constraints, traffic rules, and driving comfort. The first computed control input of the CFTOCP is fed to the system at each time step.

A. Vehicle Model

The Jerk Model is used as the EV's motion model in both longitudinal and lateral direction:

$$\underbrace{\begin{bmatrix} p_{*,k+1}^{(\mathrm{EV})} \\ v_{*,k+1}^{(\mathrm{EV})} \\ a_{*,k+1}^{(\mathrm{EV})} \end{bmatrix}}_{x_{*,k+1}^{(\mathrm{EV})}} = \underbrace{\begin{bmatrix} 1 & T_\mathrm{p} & \frac{1}{2}{T_\mathrm{p}}^2 \\ 0 & 1 & T_\mathrm{p} \\ 0 & 0 & 1 \end{bmatrix}}_{A} \underbrace{\begin{bmatrix} p_{*,k}^{(\mathrm{EV})} \\ v_{*,k}^{(\mathrm{EV})} \\ a_{*,k}^{(\mathrm{EV})} \end{bmatrix}}_{x_{*,k}^{(\mathrm{EV})}} + \underbrace{\begin{bmatrix} \frac{1}{6}{T_\mathrm{p}}^3 \\ \frac{1}{2}{T_\mathrm{p}}^2 \\ T_\mathrm{p} \end{bmatrix}}_{B} \underbrace{j_{*,k}^{(\mathrm{EV})}}_{u_{*,k}^{(\mathrm{EV})}}, \tag{13}$$

with the prediction time step T_p, which differs from the sampling time step T of the IMM-KF in this paper. (13) can be rewritten as

$$x_{k+1}^{(\mathrm{EV})} = \underbrace{\begin{bmatrix} A & 0_{3\times3} \\ 0_{3\times3} & A \end{bmatrix}}_{\bar{A}} x_k^{(\mathrm{EV})} + \underbrace{\begin{bmatrix} B \\ B \end{bmatrix}}_{\bar{B}} u_k^{(\mathrm{EV})}. \tag{14}$$

B. Scenario-based Model Predictive Controller

The proposed SCMPC scheme has two control modes: (i) the EV stays in the current lane and keeps its velocity (ii) the EV switches to the target lane and keeps its velocity. For each control mode, a CFTOCP is solved for a corresponding reference trajectory. The decision-making module then selects the control mode with the lower cost.

In addition to the generated scenarios, a so-called 'worst case' scenario is introduced to ensure the recursive feasibility of CFTOCP. In this scenario, the LV is assumed to decelerate with its minimum acceleration over the prediction horizon. We introduce two sequences of control inputs $u_0^{(\mathrm{EV})}, ..., u_{N-1}^{(\mathrm{EV})}$ and $\breve{u}_0^{(\mathrm{EV})}, ..., \breve{u}_{N-1}^{(\mathrm{EV})}$. The first input sequence is calculated to avoid collision between the EV and the LV/TVs under the generated scenarios, and used to evaluate the cost function with associated states $x_k^{(\mathrm{EV})}$. The second sequence is obtained by considering the safety constraints under the 'worst case' scenario, with associated states $\breve{x}_k^{(\mathrm{EV})}$, and the terminal set of the states $\breve{\mathbb{X}}_f^{(\mathrm{EV})}$, detailed in the proof of recursive feasibility. The first computed inputs $u_0^{(\mathrm{EV})}$ and $\breve{u}_0^{(\mathrm{EV})}$ must be equal to guarantee the recursive feasibility. The CFTOCP is formulated as

$$J = \min_{u_k^{(\mathrm{EV})}, x_{k+1}^{(\mathrm{EV})}} \sum_{k=0}^{N-1} \left\| x_{k+1}^{(\mathrm{EV})} - x_{\mathrm{ref},k+1}^{(\mathrm{EV})} \right\|_{\bar{Q}} + \left\| u_k^{(\mathrm{EV})} \right\|_{\bar{R}}, \tag{15a}$$

$$s.t. \quad x_{k+1}^{(\mathrm{EV})} = f(x_k^{(\mathrm{EV})}, u_k^{(\mathrm{EV})}), \quad k = 0, 1, ..., N-1, \tag{15b}$$

$$\breve{x}_{k+1}^{(\mathrm{EV})} = f(\breve{x}_k^{(\mathrm{EV})}, \breve{u}_k^{(\mathrm{EV})}), \quad k = 0, 1, ..., N-1, \tag{15c}$$

$$x_k^{(\mathrm{EV})} \in \mathbb{X}^{(\mathrm{EV})}, \quad \breve{x}_k^{(\mathrm{EV})} \in \breve{\mathbb{X}}^{(\mathrm{EV})}, \quad k = 0, 1, ..., N-1, \tag{15d}$$

$$u_k^{(\mathrm{EV})} \in \mathbb{U}^{(\mathrm{EV})}, \quad \breve{u}_k^{(\mathrm{EV})} \in \breve{\mathbb{U}}^{(\mathrm{EV})}, \quad k = 0, 1, ..., N-1, \tag{15e}$$

$$u_0^{(\mathrm{EV})} = \breve{u}_0^{(\mathrm{EV})}, \tag{15f}$$

$$\breve{x}_N^{(\mathrm{EV})} \in \breve{\mathbb{X}}_f^{(\mathrm{EV})}, \tag{15g}$$

$$x_0^{(\mathrm{EV})} = \breve{x}_0^{(\mathrm{EV})} = x^{(\mathrm{EV})}(0). \tag{15h}$$

Here $x_{\mathrm{ref},k+1}^{(\mathrm{EV})}$ is the reference state based on the relevant control mode. In the lane-change mode, we consider the EV only changes one lane according to the real traffic situation, so the number of related reference trajectories depends on the current lane of the EV. $\bar{Q} \in \mathbb{R}^{6\times6}$ and $\bar{R} \in \mathbb{R}^{2\times2}$ are tune-able positive definite weighting matrices. The feasible state sets $\mathbb{X}^{(\mathrm{EV})}$ and $\breve{\mathbb{X}}^{(\mathrm{EV})}$, and input set $\mathbb{U}^{(\mathrm{EV})}$ and $\breve{\mathbb{U}}^{(\mathrm{EV})}$ are limited by appropriate constraints, as detailed below.

Remark 1. If there is no LV in reality, it is assumed that there is an LV far away from the EV.

Remark 2. During the lane change of the EV, we call the lane-keeping control mode deactivated when keeping the current lane is infeasible.

C. Constraints

1) State and input constraints: The EV's motion state and action are limited by traffic rules and driving comfort. The lateral position is constrained by the lane bounds $[l_\mathrm{ub}, l_\mathrm{lb}]$

$$0 < v_{\mathrm{lon},k}^{(\mathrm{EV})}, \quad l_\mathrm{lb} \le p_{\mathrm{lat},k}^{(\mathrm{EV})} \le l_\mathrm{ub}, \tag{16a}$$

$$\underline{a}_\mathrm{lon}^{(\mathrm{EV})} \le a_{\mathrm{lon},k}^{(\mathrm{EV})} \le \overline{a}_\mathrm{lon}^{(\mathrm{EV})}, \quad \underline{a}_\mathrm{lat}^{(\mathrm{EV})} \le a_{\mathrm{lat},k}^{(\mathrm{EV})} \le \overline{a}_\mathrm{lat}^{(\mathrm{EV})}, \tag{16b}$$

$$\underline{j}_\mathrm{lon}^{(\mathrm{EV})} \le j_{\mathrm{lon},k}^{(\mathrm{EV})} \le \overline{j}_\mathrm{lon}^{(\mathrm{EV})}, \quad \underline{j}_\mathrm{lat}^{(\mathrm{EV})} \le j_{\mathrm{lat},k}^{(\mathrm{EV})} \le \overline{j}_\mathrm{lat}^{(\mathrm{EV})}, \tag{16c}$$

where $\underline{\bullet}$ and $\overline{\bullet}$ denote the minimum and maximum values of the associated variables.

2) Safety constraints: A safe distance between the EV and the preceding vehicles in the same lane is required:

$$d_k \ge \underline{d}, \tag{17}$$

and the safety distance $\underline{d}$ is computed by

$$\underline{d} = \tau v_{\mathrm{lon},k}^{(\mathrm{EV})} + \triangle d, \tag{18}$$

with the design parameters τ and $\triangle d$. If the reference point of all vehicles is in their respective center, for example, choose $\triangle d \ge \frac{l^{(\mathrm{EV})}+l^{(\mathrm{LV})}}{2}$, where $l^{(\mathrm{EV})}$ and $l^{(\mathrm{LV})}$ are the length of EV and LV. During the lane-change period, in addition to keeping a safe distance from the LVs in both the current and target lane, the EV should also maintain a safe distance with the TV behind it in the target lane. The required safety distance also satisfies (18). The safety constraint under the generated scenario is based on (18), while the safety distance for considering the 'worst case' scenario collapses to $\triangle d$.

D. Recursive Feasibility of the SCMPC

Definition 1. (**Recursive Feasibility**) The SCMPC is recursively feasible if (17) always holds. Namely, in lane-keeping mode, a collision between the EV and the LV is always avoidable. In lane-change mode, no accident occurs between the EV and the other vehicles during the lane-change process, and then the EV remains safe in the target lane.

If the safety constraints are met in the 'worst case' scenario, it means that the EV can manage any traffic situation under the SCMPC. This capability is denoted by a parameter called the minimal stopping horizon $\underline{N}$, defined as follows.

Definition 2. (**Minimal Stopping Horizon**) Given the initial velocity $v_{\mathrm{lon},0}^{(\mathrm{EV})}$ and the minimal acceleration $\underline{a}_\mathrm{lon}^{(\mathrm{EV})}$ of the EV, the minimal stopping horizon $\underline{N} \in \mathbb{N}$ satisfies

$$\underline{N} = \left\lceil \frac{v_{\mathrm{lon},0}^{(\mathrm{EV})}}{|\underline{a}_\mathrm{lon}^{(\mathrm{EV})}| T_\mathrm{p}} \right\rceil, \tag{19}$$

where $\lceil \bullet \rceil$ is defined as the smallest integer that is not smaller than a real number $\bullet$.

If we choose the prediction horizon $N \geq \underline{N}$, the terminal set $\breve{\mathbb{X}}_{\mathrm{f}}$ at the time t is

$$\breve{\mathbb{X}}_{\mathrm{f}}^{(\mathrm{EV})} \triangleq \{\breve{x}_{N|t}^{(\mathrm{EV})} | \breve{x}_{N|t}^{(\mathrm{EV})} = \begin{bmatrix} p_{\mathrm{lon},\underline{N}|t}^{(\mathrm{EV})} & 0 & 0 & p^{(\lambda)} & 0 & 0 \end{bmatrix}^{\top}\}, \tag{20}$$

where the stopping longitudinal position $p_{\mathrm{lon},\underline{N}|0}^{(\mathrm{EV})}$ of EV is determined by its initial position $p_{\mathrm{lon},0}^{(\mathrm{EV})}$, initial velocity $v_{\mathrm{lon},0}^{(\mathrm{EV})}$ and minimal acceleration $\underline{a}_{\mathrm{lon}}^{(\mathrm{EV})}$. The terminal lateral position of the EV is the position of the center line of the target lane $p^{(\lambda)}$ under the specific control mode. Based on the general traffic situation and rules, we make the following assumptions.

Assumption 1. All vehicles only drive forward, and the EV is only responsible for the front collisions.

Assumption 2. $u_k^{(\mathrm{EV})} = \begin{bmatrix} 0 & 0 \end{bmatrix}^{\top}$ is one element of the feasible set $\breve{\mathbb{U}}^{(\mathrm{EV})}$.

The recursive feasibility of the SCMPC is then proved.

Theorem 1. If SCMPC is initially feasible, and the prediction horizon $N \geq \underline{N}$, then the controller is recursively feasible based on Assumptions 1, 2.

Proof. Let two initial control inputs of the generated normal scenarios and the 'worst case' scenario be $\{u_{0|0}^{(\mathrm{EV})}, u_{1|0}^{(\mathrm{EV})}, ..., u_{\underline{N}|0}^{(\mathrm{EV})}, ..., u_{N|0}^{(\mathrm{EV})}\}$ and $\{\breve{u}_{0|0}^{(\mathrm{EV})}, \breve{u}_{1|0}^{(\mathrm{EV})}, ..., \breve{u}_{\underline{N}|0}^{(\mathrm{EV})}, ..., \breve{u}_{N|0}^{(\mathrm{EV})}\}$. Choose the second control sequence as initially feasible solution $\{\breve{u}_{0|0}^{(\mathrm{EV})\star}, \breve{u}_{1|0}^{(\mathrm{EV})\star}, ..., \breve{u}_{\underline{N}|0}^{(\mathrm{EV})\star}, ..., \breve{u}_{N|0}^{(\mathrm{EV})\star}\}$, and its related state sequence is $\{\breve{x}_{0|0}^{(\mathrm{EV})\star}, \breve{x}_{1|0}^{(\mathrm{EV})\star}, ..., \breve{x}_{\underline{N}|0}^{(\mathrm{EV})\star}, ..., \breve{x}_{N|0}^{(\mathrm{EV})\star}\}$. The terminal state $\breve{x}_{N|0}^{(\mathrm{EV})\star}$ is determined according to (20). We apply $\breve{u}_{0|0}^{(\mathrm{EV})\star}$ to the system (14), and obtain

$$x_1^{(\mathrm{EV})} = \bar{A} x_0^{(\mathrm{EV})} + \bar{B} \breve{u}_{0|0}^{(\mathrm{EV})\star} = \breve{x}_{1|0}^{(\mathrm{EV})\star}. \tag{21}$$

Then the following is a feasible solution for the MPC problem initialized at $x_1^{(\mathrm{EV})}$:

$$\begin{aligned} &\{u_{1|1}^{(\mathrm{EV})}, u_{2|1}^{(\mathrm{EV})}, ..., u_{\underline{N}|1}^{(\mathrm{EV})}, ..., u_{N-1|1}^{(\mathrm{EV})}, u_{N|1}^{(\mathrm{EV})}\} = \\ &\{\breve{u}_{1|0}^{(\mathrm{EV})\star}, \breve{u}_{2|0}^{(\mathrm{EV})\star}, ..., \breve{u}_{\underline{N}|0}^{(\mathrm{EV})\star}, ..., \breve{u}_{N-1|0}^{(\mathrm{EV})\star}, \begin{bmatrix} 0 & 0 \end{bmatrix}^{\top}\}, \end{aligned} \tag{22}$$

where $\begin{bmatrix} 0 & 0 \end{bmatrix}^{\top} \in \breve{\mathbb{U}}^{(\mathrm{EV})}$. The related state sequence is

$$\begin{aligned} &\{x_{2|1}^{(\mathrm{EV})}, x_{3|1}^{(\mathrm{EV})}, ..., x_{\underline{N}+1|1}^{(\mathrm{EV})}, ..., x_{N|1}^{(\mathrm{EV})}, x_{N+1|1}^{(\mathrm{EV})}\} = \\ &\{\breve{x}_{2|0}^{(\mathrm{EV})\star}, \breve{x}_{3|0}^{(\mathrm{EV})\star}, ..., \breve{x}_{\underline{N}|0}^{(\mathrm{EV})\star}, ..., \breve{x}_{N|0}^{(\mathrm{EV})\star}, \bar{A}\breve{x}_{N|0}^{(\mathrm{EV})\star} + \bar{B} \cdot \begin{bmatrix} 0 & 0 \end{bmatrix}^{\top}\}, \end{aligned} \tag{23}$$

where $\bar{A}\breve{x}_{N|0}^{(\mathrm{EV})\star} + \bar{B} \cdot \begin{bmatrix} 0 & 0 \end{bmatrix}^{\top} = \breve{x}_{N|0}^{(\mathrm{EV})\star}$. Both sequences are feasible for the MPC problem because they satisfy the dynamics and the constraints. □

V. SIMULATION AND DISCUSSION

The presented method is assessed with one documentation (ID:01) of the HighD dataset [15], which records the motion states of 1047 vehicles in 900s with a sampling time of 0.04s. We take two specific traffic situations as case studies, including the EV's initial motion states and the TVs' motion states during the simulation time. The designed control system directs the EV's movement in subsequent time steps.

A. Simulation Setup

Fig. 2 gives the initial scenes of case studies. Table I shows the parameters used in both cases, including the whole simulation time T_{s}. Table II shows the initial mode states of vehicles with the proper units, and the length l and width w of vehicles in two cases. Note that we only consider the EV changes to lane 1 in the lane-change mode of the simulation.

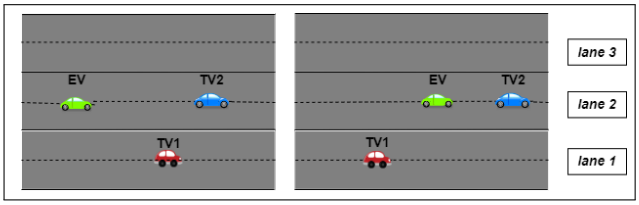

Fig. 2: The initial scenes for Case 1 (left) and Case 2 (right)

TABLE I: Design parameters used in the simulation study

Parameter	T_{s}(s)	T(s)	T_{p}(s)
Value	10.00	0.04	0.40
Parameter	N	$\underline{a}_{\mathrm{lon}}^{(\mathrm{EV})}$(m/s^2)	$\overline{a}_{\mathrm{lon}}^{(\mathrm{EV})}$(m/s^2)
Value	15	-4.00	4.00
Parameter	$\underline{a}_{\mathrm{lat}}^{(\mathrm{EV})}$(m/s^2)	$\overline{a}_{\mathrm{lat}}^{(\mathrm{EV})}$(m/s^2)	$j_{\mathrm{lon}}^{(\mathrm{EV})}$(m/s^2)
Value	-4.00	4.00	-5.00
Parameter	$\overline{j}_{\mathrm{lon}}^{(\mathrm{EV})}$(m/s^2)	$\underline{j}_{\mathrm{lat}}^{(\mathrm{EV})}$(m/s^2)	$\overline{j}_{\mathrm{lat}}^{(\mathrm{EV})}$(m/s^2)
Value	5.00	-4.00	4.00
Parameter	τ(s)	l_{ub}(m)	l_{lb}(m)
Value	0.40	33.80	21.00
Parameter	$p_{\mathrm{c}}^{(1),(2),(3)}$(m)	K_{lat}	$\underline{a}_{\mathrm{lon}}^{(\mathrm{LV})}$(m/s^2)
Value	$\{22.98, 26.88, 31.3\}$	$[1.15, 3.39, 3.58]^{\top}$	-3.00

TABLE II: States initial values and vehicle parameters

Case 1		
Parameter	$\{p_{\mathrm{lon},0}, v_{\mathrm{lon},0}, a_{\mathrm{lon},0}, p_{\mathrm{lat},0}, v_{\mathrm{lat},0}, a_{\mathrm{lat},0}\}$	$\{l, w\}$
EV	$\{2.84, 34.8, 0.27, 25.65, -0.09, -0.01\}$	$\{4.85, 2.02\}$
TV1	$\{127.87, 32.74, 0.13, 21.52, -0.21, 0.2\}$	$\{5.96, 2.32\}$
TV2	$\{141.19, 23.04, 0.05, 25.42, 0.1, -0.03\}$	$\{14.35, 2.5\}$
Case 2		
Parameter	$\{p_{\mathrm{lon},0}, v_{\mathrm{lon},0}, a_{\mathrm{lon},0}, p_{\mathrm{lat},0}, v_{\mathrm{lat},0}, a_{\mathrm{lat},0}\}$	$\{l, w\}$
EV	$\{181.5, 25.07, -0.29, 25.49, 0.09, -0.01\}$	$\{4.14, 1.92\}$
TV1	$\{151.54, 32.59, 0.28, 22.21, -0.27, 0.01\}$	$\{4.75, 2.02\}$
TV2	$\{201.31, 23.21, 0.17, 25.62, 0.17, -0.02\}$	$\{9.2, 2.5\}$

B. Simulation Results

Figs. 3 and 8 show the open-loop trajectories of the EV over time, the closed-loop trajectory of the EV, and the TVs' trajectory in two cases.

1) Case 1: The velocity profile of all vehicles over the entire sampling time is shown in Fig. 4. Fig. 5 displays the cost function value of two controllers. The cost of the SCMPC is set as an arbitrary big value when it is deactivated,

like 5000. As Fig. 5 shows, between 0s and 7.6s, lane-keeping is the desirable maneuver. Between 0s and 4s, the EV keeps its velocity and then decelerates until around 7.6s to have a safe distance from TV2. After that, at 7.6s, the cost of changing lanes becomes lower, prompting the EV to initiate a lane-change maneuver. After about 1.5s, the lane-change maneuver succeeds. Then, the EV maintains a constant velocity in its new lane for the remaining time steps, while the lane change becomes too costly and impossible at around 11.8s. In particular, the increasing values between 9.2s and 11.8s lead to a visual discontinuity in the lane-change cost-function curve, the largest of which reaches a value of 56000.

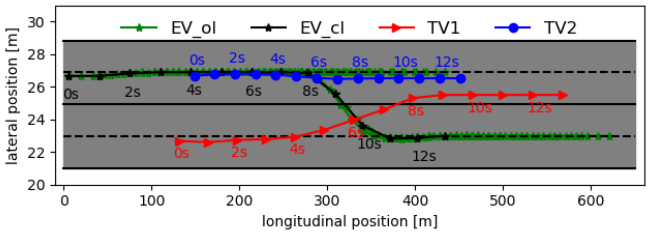

Fig. 3: The motion trajectory of vehicles in Case 1

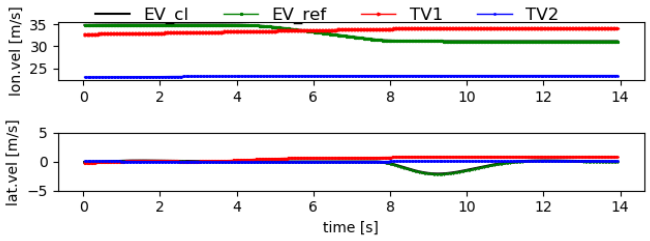

Fig. 4: The velocity profile in Case 1

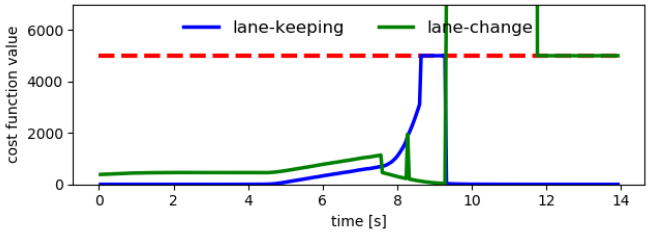

Fig. 5: The cost function value of controllers in Case 1

Fig. 6 and 7 illustrate traffic prediction results for Case 1 at 5s and 9s. At 5s, three scenarios are generated: TV1 performs a VT maneuver in lane 1 (black edge), or lane 2 (blue edge), and TV2 performs VT maneuvers in lane 1 (red edge), or lane 2 (blue edge). The associated probabilities are $\{\mu_1^{(1)}\mu_2^{(2)}, \mu_2^{(1)}\mu_1^{(2)}, \mu_2^{(1)}\mu_2^{(2)}\} = \{0.241, 0.186, 0.573\}$. At 9s, TV1 may perform a VT maneuver in lane 2 (black edge), or lane 3 (magenta edge), and TV2 may perform a VT maneuver in lane 2 (black edge). The associated probabilities are $\{\mu_2^{(1)}\mu_2^{(2)}, \mu_3^{(1)}\mu_2^{(2)}\} = \{0.913, 0.087\}$.

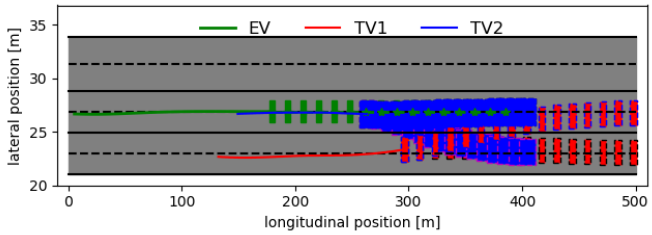

Fig. 6: Traffic prediction at 5s in Case 1

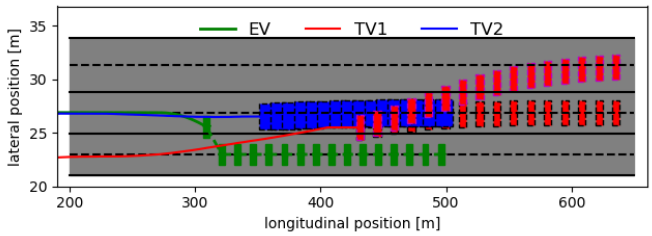

Fig. 7: Traffic prediction at 9s in Case 1

2) Case 2: The vehicles' motion trajectories, velocity profile, and the cost function value of two SCMPCs are displayed in Figs. 8, 9 and 10. From 0s to 2s, the EV maintains its speed under the control strategy, but the cost rises continuously. This is because it is impossible to maintain a safe distance from TV2, while consistently keeping a higher velocity throughout the prediction horizon. Since then, the EV starts to reduce its speed to the speed of TV2 until 4s, which accordingly leads to a decrease in the value of the cost function. Note that the lane-change becomes available after about 5s, before which we set its associated cost function value as 5000. After that, its cost remains higher than lane-keeping. Therefore, the EV stays in the current lane in the following time steps.

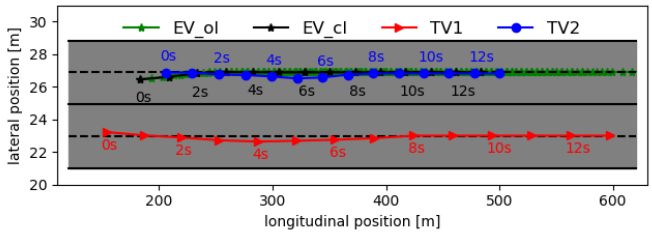

Fig. 8: The motion trajectory of vehicles in Case 2

The traffic prediction results for Case 2 at 3s and 6s are shown in Figs. 11 and 12. At 3s, two scenarios are generated: TV1 performs a VT maneuver in lane 1 (black edge), or lane 2 (white edge), and TV2 performs a VT maneuver in lane 2 (black edge). The associated probabilities are $\{\mu_1^{(1)}\mu_2^{(2)}, \mu_2^{(1)}\mu_2^{(2)}\} = \{0.860, 0.140\}$. At 6s, three scenarios are generated: TV1 performs a VT maneuver in lane 1 (black edge), and TV2 performs a VT maneuver in lane 1 (black edge), lane 2 (white edge), or lane 3 (blue edge).

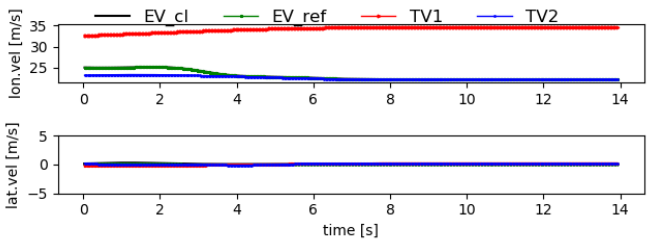

Fig. 9: The velocity profile in Case 2

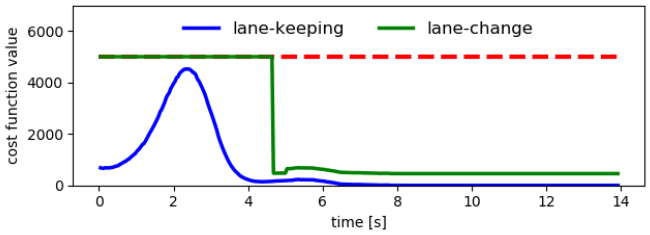

Fig. 10: The cost function value of controllers in Case 2

The related probabilities are $\{\mu_1^{(1)}\mu_1^{(2)}, \mu_1^{(1)}\mu_2^{(2)}, \mu_1^{(1)}\mu_3^{(2)}\} = \{0.130, 0.727, 0.143\}$.

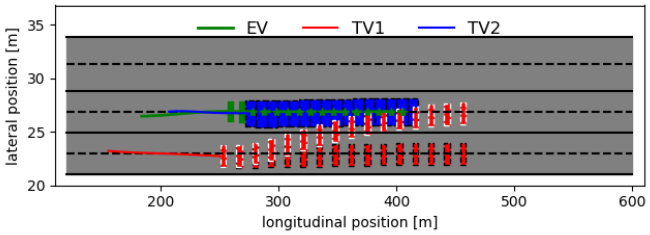

Fig. 11: Traffic prediction at 3s in Case 2

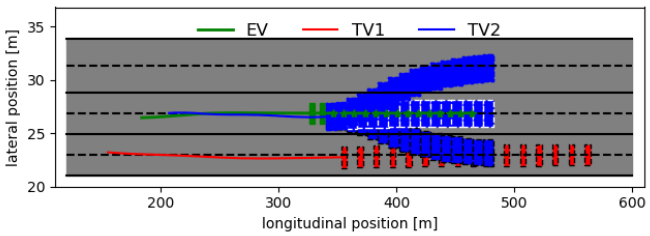

Fig. 12: Traffic prediction at 6s in Case 2

Simulation results of Cases 1 and 2 indicate that the EV executes safe maneuvers under the designed control structure while considering the interaction with other vehicles.

VI. SUMMARY AND FUTURE WORK

The paper investigates the interaction-aware state estimation of the vehicles using IMM-KF and represents the uncertain environment through related state prediction with probability. The generated scenarios, along with the 'worst case' scenario, are used to formulate the safety constraints of the SCMPC. The control input with lower cost among the lane-keeping and lane-change modes is applied to the system. Moreover, the system's recursive feasibility is ensured by preventing collision between the EV and the LV in a 'worst case' scenario. The proposed algorithm is validated for two highway scenes from the HighD dataset. Simulation results demonstrate the capability of the proposed control method to perform safe maneuvers. Validating the proposed structure in a high-fidelity environment to include the reactions of TVs to the EV in time is the subject of future work.

REFERENCES

[1] C. Gkartzonikas and K. Gkritza, "What have we learned? a review of stated preference and choice studies on autonomous vehicles," *Transportation Research Part C: Emerging Technologies*, vol. 98, pp. 323–337, 2019.

[2] S. Lefèvre, D. Vasquez, and C. Laugier, "A survey on motion prediction and risk assessment for intelligent vehicles," *ROBOMECH journal*, vol. 1, no. 1, pp. 1–14, 2014.

[3] J. Zhou, B. Olofsson, and E. Frisk, "Interaction-aware moving target model predictive control for autonomous vehicles motion planning," in *2022 European Control Conference (ECC)*, 2022, pp. 154–161.

[4] G. Cesari, G. Schildbach, A. Carvalho, and F. Borrelli, "Scenario model predictive control for lane change assistance and autonomous driving on highways," *IEEE Intelligent transportation systems magazine*, vol. 9, no. 3, pp. 23–35, 2017.

[5] M. Bichi, G. Ripaccioli, S. Di Cairano, D. Bernardini, A. Bemporad, and I. V. Kolmanovsky, "Stochastic model predictive control with driver behavior learning for improved powertrain control," in *49th IEEE conference on decision and control (CDC)*. IEEE, 2010, pp. 6077–6082.

[6] S. H. Nair, V. Govindarajan, T. Lin, Y. Wang, E. H. Tseng, and F. Borrelli, "Stochastic mpc with dual control for autonomous driving with multi-modal interaction-aware predictions," *arXiv preprint arXiv:2208.03525*, 2022.

[7] Y. Chen, U. Rosolia, C. Fan, A. Ames, and R. Murray, "Reactive motion planning with probabilisticsafety guarantees," in *Conference on robot learning*. PMLR, 2021, pp. 1958–1970.

[8] Y. Chen, U. Rosolia, W. Ubellacker, N. Csomay-Shanklin, and A. D. Ames, "Interactive multi-modal motion planning with branch model predictive control," *IEEE Robotics and Automation Letters*, vol. 7, no. 2, pp. 5365–5372, 2022.

[9] B. Ivanovic, A. Elhafsi, G. Rosman, A. Gaidon, and M. Pavone, "Mats: An interpretable trajectory forecasting representation for planning and control," *arXiv preprint arXiv:2009.07517*, 2020.

[10] M. A. Perez, J. D. Sudweeks, E. Sears, J. Antin, S. Lee, J. M. Hankey, and T. A. Dingus, "Performance of basic kinematic thresholds in the identification of crash and near-crash events within naturalistic driving data," *Accident Analysis & Prevention*, vol. 103, pp. 10–19, 2017.

[11] Y. He, B. Ciuffo, Q. Zhou, M. Makridis, K. Mattas, J. Li, Z. Li, F. Yan, and H. Xu, "Adaptive cruise control strategies implemented on experimental vehicles: A review," *IFAC-PapersOnLine*, vol. 52, no. 5, pp. 21–27, 2019.

[12] S. Magdici and M. Althoff, "Adaptive cruise control with safety guarantees for autonomous vehicles," *IFAC-PapersOnLine*, vol. 50, no. 1, pp. 5774–5781, 2017.

[13] X. Xu, X. Wang, X. Wu, O. Hassanin, and C. Chai, "Calibration and evaluation of the responsibility-sensitive safety model of autonomous car-following maneuvers using naturalistic driving study data," *Transportation research part C: emerging technologies*, vol. 123, p. 102988, 2021.

[14] V. Lefkopoulos, M. Menner, A. Domahidi, and M. N. Zeilinger, "Interaction-aware motion prediction for autonomous driving: A multiple model kalman filtering scheme," *IEEE Robotics and Automation Letters*, vol. 6, no. 1, pp. 80–87, 2020.

[15] R. Krajewski, J. Bock, L. Kloeker, and L. Eckstein, "The highd dataset: A drone dataset of naturalistic vehicle trajectories on german highways for validation of highly automated driving systems," in *2018 21st International Conference on Intelligent Transportation Systems (ITSC)*, 2018, pp. 2118–2125.